

**Center-of-mass quantization of excitons in PbI<sub>2</sub> thin films grown by vacuum deposition**

M. Nakayama\* and D. Kim

*Department of Applied Physics, Graduate School of Engineering, Osaka City University, 3-3-138 Sugimoto, Sumiyoshi-ku, Osaka 558-8585, Japan*

H. Ishihara†

*Department of Physics and Electronics, Graduate School of Engineering, Osaka Prefecture University, 1-1 Gakuen-cho, Naka-ku, Sakai, Osaka 599-8531, Japan*

(Received 12 January 2006; published 18 August 2006)

We have investigated excitonic properties of PbI<sub>2</sub> thin films grown on a (001) NaCl substrate by a conventional vacuum deposition technique. The x-ray-diffraction patterns indicate that the crystal structure of the PbI<sub>2</sub> thin films is just oriented along the [001] crystal axis. The surface morphology observed by an atomic force microscope shows that the surface roughness is within 1 nm. These results of the structural analysis demonstrate that the PbI<sub>2</sub> thin films are suitable for the investigation of quantization effects. The absorption spectra of 8-, 10-, and 15-nm-thick films clearly exhibit oscillatory structures in the energy region higher than the fundamental exciton transition up to  $\sim 110$  meV. This fact indicates the nice realization of the center-of-mass quantization of the exciton; however, the usually used model that is the wave-vector quantization of a parabolic exciton band could not be reasonably applied to explain the quantized exciton energies. The absorption spectra are quantitatively analyzed on the basis of a tight-binding exciton model for the energy dispersion using a nonlocal theory of linear optical response.

DOI: [10.1103/PhysRevB.74.073306](https://doi.org/10.1103/PhysRevB.74.073306)

PACS number(s): 73.21.-b, 78.66.Li, 78.40.Fy

Quantization effects on excitons have attracted considerable attention in optical properties and functions of semiconductors. It is well known that the quantization effects are classified into two types. One is individual quantization of envelope functions of electrons and holes in the case in which an excitonic Bohr radius is larger than a spatial confinement size, which is a typical phenomenon in ordinary quantum-well systems and has been extensively studied until now. The other is center-of-mass (c.m.) quantization of excitons, which corresponds to quantization of the translational motion, when the exciton is weakly confined in substance space larger than the Bohr radius. The investigation of the c.m. quantization has not been so active, thus there are limited numbers of relevant reports: e.g., thin films of GaAs,<sup>1-3</sup> CdTe,<sup>4,5</sup> CuCl,<sup>6,7</sup> and layered compounds such as WSe<sub>2</sub> (Ref. 8) and PbI<sub>2</sub>.<sup>9,10</sup> The c.m. quantization, however, has been recently highlighted for nonlinear optical responses by the development of the nonlocal theory of interactions between weakly confined excitons and photons.<sup>11</sup> For example, a large third-order nonlinear response induced by the nonlocality in GaAs thin films was demonstrated,<sup>3,12</sup> and optical bistability due to the spatial structure of an internal electric field in a nanoscale film was proposed.<sup>13</sup>

Layered compounds are good candidates for c.m. quantization because the exciton binding energy is usually high, and the lattice interaction along the *c* axis is a van der Waals force, which results in a considerable merit for the thin-film growth. PbI<sub>2</sub> is a typical layered compound, and its exciton binding energy and Bohr radius are suitable for the c.m. quantization: 63 meV and 1.9 nm, respectively.<sup>14</sup> Saito and Goto<sup>10</sup> precisely studied the quantization effects on excitons in PbI<sub>2</sub> microcrystallites with an ultrathin thickness from two to eight unit layers, where the unit layer corresponds to the lattice-stacking unit along the *c* axis: 0.698 nm.<sup>15</sup> They concluded that the framework of the c.m. quantization is approved in the layer thickness larger than five unit layers;

however, only the first quantized ( $n=1$ ) state was observed owing to fluctuations of microcrystallite thickness. The most prominent feature of the c.m. quantization is the appearance of oscillatory structures of absorption (transmission) and reflection spectra originated from quantized states with  $n \geq 2$ , which is characterized by the wave-vector quantization of  $K_n = n\pi/L$ : *L* is a film thickness. From an aspect of the exciton stability, CuCl is the best candidate for the c.m. quantization: the very high exciton binding energy of  $\sim 190$  meV and the very small Bohr radius of  $\sim 0.7$  nm.<sup>7</sup> In fact, oscillatory structures reflecting the c.m. quantization were clearly observed in CuCl thin films;<sup>6,7</sup> however, it should be noted that CuCl is a hygroscopic material, which leads to remarkable degradation of crystal quality.

In the present work, we have investigated the c.m. quantization effect on excitons in PbI<sub>2</sub> thin films with a layer thickness from 8 to 50 nm grown by a conventional vacuum deposition method. The structural characterization of the thin films with an x-ray diffraction method and an atomic force microscope indicates the high crystal quality and very smooth surface. The absorption spectra in the 8-, 10-, and 15-nm-thick films clearly exhibit oscillatory structures reflecting the c.m. quantization. It is noted that the observed energies of the quantized excitons could not be explained by the quantization of the parabolic exciton band, the so-called effective-mass approximation, usually adopted in the analysis of the c.m. quantization. Here, we quantitatively analyze the absorption spectra on the basis of a tight-binding exciton model allowing the nearest-neighbor energy transfer in the framework of the nonlocal theory of linear optical response.<sup>16</sup>

For the sample preparation, thin films of PbI<sub>2</sub> were grown on a cleaved (001) NaCl substrate at 150 °C using a vacuum deposition method in high vacuum ( $\sim 1 \times 10^{-4}$  Pa). Commercially supplied powders of PbI<sub>2</sub> with a purity of 99.99%

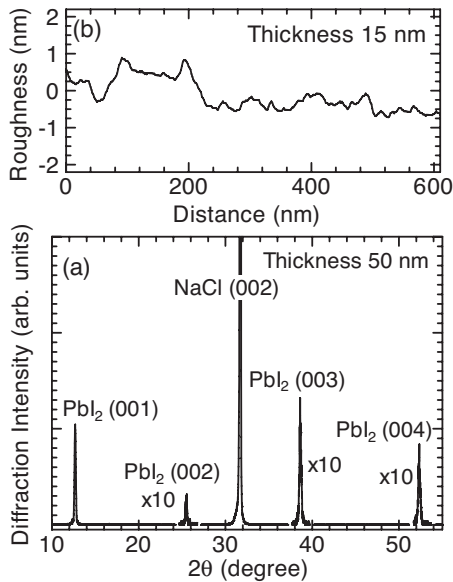


FIG. 1. (a) X-ray-diffraction pattern of the 50-nm-thick film of  $\text{PbI}_2$ , and (b) the surface-roughness profile of the 15-nm-thick film measured with the atomic force microscope under the atmospheric condition.

were heated in an alumina crucible, and the deposition rate, which was monitored by a crystal oscillator, was 0.05 nm/s. We prepared four thin films with 8, 10, 15, and 50 nm thickness. The error of the film thickness is around 1 nm. The crystal quality and surface morphology of the samples were characterized with a  $\theta$ - $2\theta$  x-ray-diffraction method and an atomic force microscope, respectively. In order to detect the optical transitions of quantized excitons, absorption spectra were measured at 10 K using a double-beam spectrometer with a resolution of 0.2 nm.

First, we describe the structural characterization of  $\text{PbI}_2$  thin films. Figure 1(a) shows the x-ray-diffraction pattern of the 50-nm-thick film with use of the  $\text{Cu } K\alpha$  line. Since the crystal structure of  $\text{PbI}_2$  has polytypism, the basic structure of  $2H$  is adapted as the criterion for the assignment of the Bragg reflections, where the lattice constants of the in-plane and  $c$  axes in the  $2H$  structure are 0.4557 and 0.6979 nm, respectively.<sup>15</sup> The in-plane ( $c$ -axis) lattice constant of the  $4H$  structure is the same (just twice) as that of  $2H$ .<sup>15</sup> The assignment of the polytypism will be discussed later with the excitonic absorption spectra. The calculated  $2\theta$  angles of the (001), (002), (003), and (004) planes are  $12.68^\circ$ ,  $25.51^\circ$ ,  $38.68^\circ$ , and  $52.41^\circ$ , respectively, so that all the Bragg reflections observed are clearly attributed to the  $(00n)$  plane. Thus, the x-ray-diffraction pattern indicates that the lattice structure of the thin film is fully oriented along the  $c$  axis. Figure 1(b) shows the surface-roughness profile of the 15-nm-thick film measured with the atomic force microscope under the atmospheric condition. It is obvious that the roughness is within 1 nm, which is comparable to the unit-layer fluctuation corresponding to the roughness limit in the thin-film growth. The very smooth surface is essential to investigate the c.m. quantization effect that is sensitive to thickness fluctuations. The results of the structural characterization described above demonstrate the merit of the layered compound for the thin-film growth.

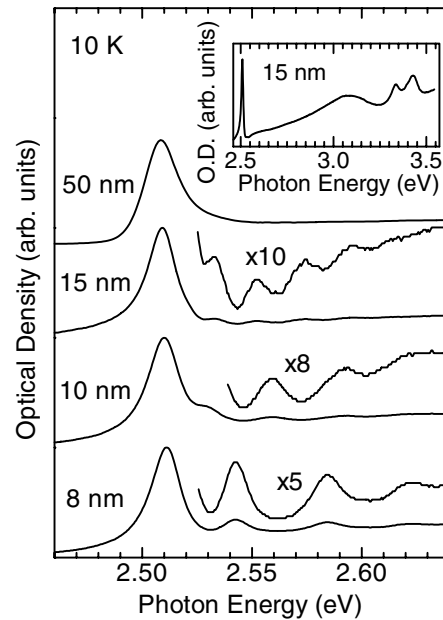


FIG. 2. Absorption spectra of the 8-, 10-, 15-, and 50-nm-thick films of  $\text{PbI}_2$  in the energy region of the fundamental exciton energy at 10 K, where the main spectrum in each thin film is normalized by the first peak intensity. The inset depicts the absorption spectrum of the 15-nm-thick film in the energy region up to 3.55 eV.

Figure 2 shows the absorption spectra of the 8-, 10-, 15-, and 50-nm-thick films of  $\text{PbI}_2$  in the energy region of the fundamental exciton transition at 10 K, where the main spectrum of each thin film is normalized by the first peak intensity. The inset depicts the absorption spectrum of the 15-nm-thick film in the energy region up to 3.55 eV. For the assignment of the polytype structure of the thin films, the most prominent difference of the excitonic properties in the  $2H$  and  $4H$  structures appears in the energy region from 3.3 to 3.45 eV.<sup>15</sup> In the  $2H$  structure, only one excitonic transition of  $A_4^+ \rightarrow A_{5+6}^-$  is observed at 3.31 eV. On the other hand, the  $A_4^+ \rightarrow A_{5+6}^-$  transition is split into two transitions of  $\Gamma_8(1) \rightarrow \Gamma_9(1)$  and  $\Gamma_8(1) \rightarrow \Gamma_9(2)$  in the  $4H$  structure by the symmetry change from  $2H$ , where the reported transition energies are 3.330 and 3.425 eV, respectively, and the notations of the excitonic transitions are taken from Ref. 15. It is evident from the inset of Fig. 2 that the doublet peaks appear at 3.331 and 3.426 eV. This spectral profile is observed in all the thin films. Thus, the crystal structure of the thin films is attributed to  $4H$ .

In the energy region of the fundamental exciton transition, the oscillatory absorption structures reflecting the c.m. quantization are clearly observed in the 8-, 10-, and 15-nm-thick films. In the 50-nm-thick film, where there is no oscillatory structure, the peak energy of the excitonic transition, 2.508 eV, just agrees with the reported energy of the fundamental exciton of the  $4H$  structure, 2.508 eV.<sup>15</sup> In order to quantitatively discuss the c.m. quantization effect, we compare the oscillatory profiles of the absorption spectra in the 8-, 10-, and 15-nm-thick films with the exciton-polariton dispersion as shown in Fig. 3. In the calculation of the polariton dispersion, the following well-known equation is used:

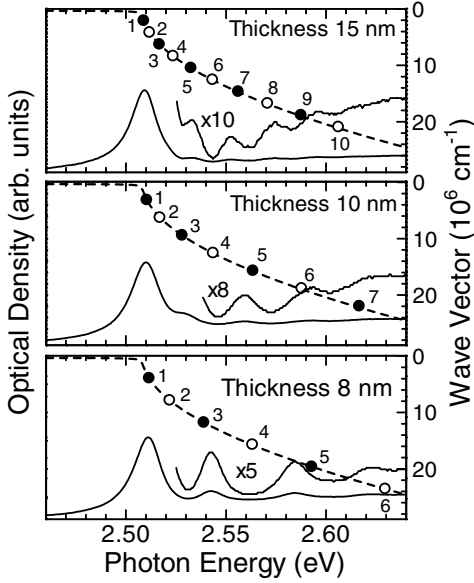


FIG. 3. Oscillatory profiles of the absorption spectra in the 8-, 10-, and 15-nm-thick films of  $\text{PbI}_2$ , and the exciton-polariton dispersion (dashed curves) calculated using  $M_{\text{ex}}=1.7m_0$ . The circles plotted on the polariton dispersion indicate the energy positions of the quantized states with the wave vector of  $K_n=n\pi/L$  in the framework of the c.m. quantization of the parabolic band, where the closed and open circles correspond to the odd and even quantum-number states, respectively.

$$\frac{c^2\hbar^2K^2}{E^2} = \varepsilon(E, K) = \varepsilon_b \left( 1 + \frac{f}{E_T^2 + E_T\hbar^2K^2/M_{\text{ex}}^2 - E^2 - iE\Gamma} \right), \quad (1)$$

where  $c$  is the speed of light in vacuum,  $K$  is the wave vector of the dispersion,  $\varepsilon_b$  is the background dielectric constant,  $E_T$  is the transverse exciton energy,  $M_{\text{ex}}$  is the translational mass of the exciton, and  $f$  is the oscillator strength. We set  $f$  to  $E_L^2 - E_T^2$  and  $\Gamma$  to zero in the calculation, where  $E_L$  is the longitudinal exciton energy. The parameters of the dielectric function are taken from Ref. 17 except for  $M_{\text{ex}}$ . In Ref. 17, interference phenomena of the exciton polariton in thin platelets of  $4H\text{-PbI}_2$  are discussed from the analysis of reflection spectra. Although the suggested value of  $M_{\text{ex}}$  is  $(1.0 \pm 0.2)m_0$ ,<sup>17</sup> we could not fit the peak energies even for the quantized excitons with  $n=3$  using that value. Thus,  $M_{\text{ex}}$  is treated as an adjustable parameter. In Fig. 3, the exciton-polariton dispersion calculated using  $M_{\text{ex}}=1.7m_0$  is depicted by the dashed curves. The circles plotted on the polariton dispersion indicate the energy positions of the quantized states with the wave vector of  $K_n=n\pi/L$  in the framework of the c.m. quantization, where the closed and open circles correspond to the odd and even quantum-number states, respectively. The calculated results of the quantized exciton energies agree fairly well with the experimental results. The energy range of the observation of the c.m. quantization is  $\sim 110$  meV in the  $\text{PbI}_2$  thin films. It is noted that the energy range of the c.m. quantization is  $\sim 30$  meV even in  $\text{CuCl}$  thin films.<sup>6,7</sup> Comparing the oscillatory structures and the exciton-polariton dispersion in Fig. 3, we notice that the odd quantum-number states are mainly observed. This is an ordi-

nary consequence of the selection rule of the excitonic transition under the c.m. quantization condition based on a long-wavelength approximation (LWA), which is well confirmed by the previous reports on  $\text{CuCl}$  thin films.<sup>6,7</sup> The basic problem in this case is that some quantized excitons in the energy region higher than  $\sim 2.57$  eV must be assigned to even quantum-number states that are fundamentally forbidden in the dipole transition. This fact suggests that the wave-vector quantization considering the parabolic dispersion of the exciton, the so-called effective-mass approximation, is inadequate.

In order to explain the absorption spectra quantitatively, we calculated the linear optical response on the basis of the tight-binding exciton model allowing the nearest-neighbor energy transfer in the framework of the nonlocal theory.<sup>16</sup> It should be noted that we could never explain the entire absorption spectra, assuming a parabolic dispersion with any effective mass. The calculation of the band structure based on an empirical pseudopotential method<sup>18</sup> suggests that the band-edge transitions of  $\text{PbI}_2$  are cationic, i.e., considerably localized orbital, which suggests that the tight-binding exciton model is an appropriate approximation for the energy dispersion. According to Ref. 16, the eigenfunction and energy dispersion of one exciton state with a set of discrete lattices can be written as

$$|K_n\rangle = \left( \frac{2}{N+1} \right)^{1/2} \sum_j \sin(K_n j) a_j^\dagger |0\rangle \quad (2)$$

and

$$E(n) = \varepsilon_0 - 2t \cos(K_n), \quad (3)$$

respectively, where  $a_j^\dagger$  is the creation operator of an exciton on the  $j$ th site,  $\varepsilon_0$  is the excitation energy of each site,  $t$  is the transfer energy that is a fitting parameter, and  $K_n$  is the allowed wave vector defined as  $K_n=n\pi/(N+1)$  with  $\{n=1, 2, \dots, N\}$ . In the calculation, the lattice spacing and lowest energy of the exciton dispersion are set to 0.698 nm and 2.5073 eV, respectively. The linear nonlocal polarization at a frequency of  $\omega$  is given by the following explicit form:<sup>16</sup>

$$P_j^{(1)}(\omega) = \frac{M^2}{v_0} \left( \frac{2}{N+1} \right)^{1/2} \sum_n \frac{\sin(K_n j) F_n}{E(n) - \omega - i\Gamma} \exp(-i\omega t). \quad (4)$$

Here,  $M$  is the transition dipole matrix per site,  $v_0$  is the unit-cell volume, and  $\Gamma$  is the phenomenological constant for response damping. The definition of  $F_n$  is described in Ref. 16. In addition, we take account of a dead-layer thickness, which is also phenomenologically treated as a fitting parameter, leading to an effective layer thickness. In the calculation of absorption spectra, the background dielectric constant and the  $L$ - $T$  splitting energy of the exciton are taken from Ref. 17.

Figure 4 shows the calculated absorption spectra of the 8-, 10-, and 15-nm-thick films on the basis of the theoretical model described above, where the spectrum intensity is normalized by the maximum value, and the arrows indicate the quantized-exciton energies taken from the experimental absorption spectra. It is obvious that the calculated energies of the quantized excitons agree fully with the experimental re-

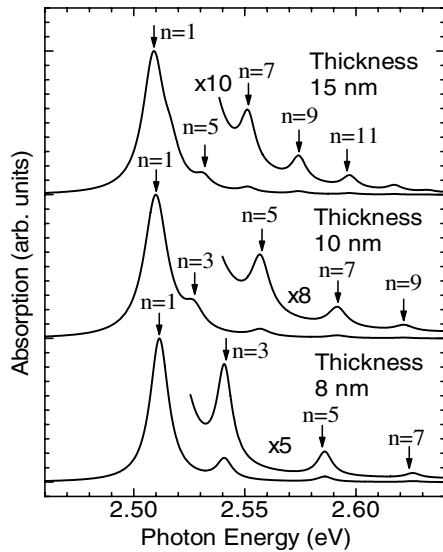


FIG. 4. Calculated absorption spectra of the 8-, 10-, and 15-nm-thick films on the basis of the tight-binding exciton model for the exciton dispersion by using the nonlocal theory of linear optical response, where the spectrum intensity is normalized by the maximum value, and the integer denotes the quantum number of the observed exciton state. The arrows indicate the energies of the quantized excitons taken from the experimental absorption spectra.

sults. The integer in Fig. 4 denotes the quantum number of the exciton state. All the observed exciton states have odd quantum numbers, which is consistent with the picture of the LWA. In the 15-nm-thick film, the missing  $n=3$  transition is covered with the tail of the absorption band of the  $n=1$  transition owing to the small energy spacing of  $\sim 7$  meV. The calculation does not take account of the continuum transitions. In the 10- and 15-nm-thick films, the oscillatory strengths of the quantized excitons with higher quantum numbers are considerably low; therefore, the background absorption due to the continuum transitions in the energy region above  $\sim 2.56$  eV becomes remarkable in comparison with that in the 8-nm-thick film. In the calculation, the fitting parameter of the transfer energy,  $t$ , is fixed to 0.0335 eV. This transfer energy corresponds to the effective mass of  $M_{\text{ex}}=2.33m_0$ , which is evaluated from the coefficient of the

second expansion term of  $2t \cos(K_n)$ . Other fitting parameters of the dead-layer thickness ( $L_d$ ) and broadening factor ( $\Gamma$ ) are as follows:  $\{L_d, \Gamma\} = \{0.86 \text{ nm}, 4.0 \text{ meV}\}$ ,  $\{0.81 \text{ nm}, 5.0 \text{ meV}\}$ , and  $\{1.22 \text{ nm}, 4.0 \text{ meV}\}$  for the 8-, 10-, and 15-nm-thick films, respectively. The dead-layer thicknesses in the 8- and 10-nm-thick films almost correspond to the unit-layer thickness, which seems to be an appropriate value. In the 15-nm-thick film, the dead-layer thickness is slightly larger than those in the 8- and 10-nm-thick films. This difference of the dead-layer thickness may be due to a slight deviation of the layer thickness from the designed value. We note that the transfer energy is the phenomenological parameter because the dispersion relation of the exciton band is not revealed; therefore, it is difficult to determine the conclusive value. Anyway, it is evident that the tight-binding exciton model leading to the cosine-type energy dispersion instead of the parabolic dispersion enables us to reasonably analyze the c.m. quantization of the exciton in the  $\text{PbI}_2$  thin films. This fact suggests that the tight-binding exciton model is applicable to the analysis of the c.m. quantization in thin films of various layered compounds and molecular crystals.

In conclusion, we have demonstrated that the c.m. quantization of the exciton is realized in the 8-, 10-, and 15-nm-thick films of  $\text{PbI}_2$  grown by the conventional vacuum deposition method owing to the merit of the layered compound, i.e., a van der Waals interaction along the  $c$  axis, which leads to the growth of the high-quality thin films with the very smooth surface: the roughness within 1 nm. The oscillatory profiles of the absorption spectra, which result from the c.m. quantization, are clearly observed. However, we could not explain the spectral profiles by the wave-vector quantization,  $K_n = n\pi/L$ , of the exciton-polariton dispersion with parabolicity. The calculation of the nonlocal linear optical response on the basis of the tight-binding exciton model for the exciton dispersion produces the reasonable absorption spectra of the quantized excitons.

This research was supported by a Grant-in-Aid for Creative Scientific Research from the Japan Society for the Promotion of Science. The authors are grateful to S. Uegaki for his help with the experiments.

\*Electronic address: nakayama@phys.eng.osaka-cu.ac.jp

†Also at CREST, Japan Science and Technology Agency, 4-1-8 Honcho, Kawaguchi, Saitama 332-0012, Japan.

<sup>1</sup>J. Kusano *et al.*, Solid State Commun. **72**, 215 (1989).

<sup>2</sup>A. Tredicucci *et al.*, Phys. Rev. B **47**, 10348 (1993).

<sup>3</sup>K. Akiyama *et al.*, Appl. Phys. Lett. **75**, 475 (1999).

<sup>4</sup>H. Tuffigo *et al.*, Phys. Rev. B **37**, 4310 (1988).

<sup>5</sup>A. D'Andrea *et al.*, Europhys. Lett. **11**, 169 (1990).

<sup>6</sup>Z. K. Tang *et al.*, Phys. Rev. Lett. **71**, 1431 (1993).

<sup>7</sup>Z. K. Tang *et al.*, Phys. Rev. B **52**, 2640 (1995).

<sup>8</sup>F. Consandori and R. F. Frindt, Phys. Rev. B **2**, 4893 (1970).

<sup>9</sup>V. K. Miloslavskii *et al.*, Fiz. Tverd. Tela (Leningrad) **17**, 1150

(1975) [Sov. Phys. Solid State **17**, 733 (1975)].

<sup>10</sup>S. Saito and T. Goto, Phys. Rev. B **52**, 5929 (1995).

<sup>11</sup>For a review, see K. Cho, *Optical Response of Nanostructures* (Springer, Berlin, 2003).

<sup>12</sup>H. Ishihara *et al.*, Phys. Rev. Lett. **89**, 017402 (2002).

<sup>13</sup>H. Ishihara, Phys. Rev. B **67**, 113302 (2003).

<sup>14</sup>Y. Nagamune *et al.*, Phys. Rev. B **40**, 8099 (1989).

<sup>15</sup>E. Doni *et al.*, Phys. Status Solidi B **68**, 569 (1975).

<sup>16</sup>H. Ishihara *et al.*, Phys. Rev. B **65**, 035305 (2002).

<sup>17</sup>T. Hayashi, J. Phys. Soc. Jpn. **55**, 2043 (1986).

<sup>18</sup>I. Ch. Schlüter and M. Schlüter, Phys. Rev. B **9**, 1652 (1974).